Mechanics of Materials 81 (2015) 72–83

Contents lists available at ScienceDirect

Mechanics of Materials

journal homepage: www.elsevier.com/locate/mechmat

Origin of stress overshoot in amorphous solids

M.Q. Jiang [a,b,*], G. Wilde [b], L.H. Dai [a]

[a] State Key Laboratory of Nonlinear Mechanics, Institute of Mechanics, Chinese Academy of Sciences, Beijing 100190, China
[b] Institute of Materials Physics, Westfälische Wilhelms-Universität Münster, Münster 48149, Germany

ARTICLE INFO

Article history:
Received 12 May 2014
Received in revised form 11 September 2014
Available online 28 October 2014

Keywords:
Amorphous solid
Plastic flow
Stress overshoot
Shear transformation zone
Free volume

ABSTRACT

Based on the shear-transformation-zone (STZ) theory, we propose a constitutive model for describing homogeneous elastoplastic deformation of amorphous solids where the interaction of shear transformations and free volume dynamics is incorporated. This theoretical model can reproduce the stress overshoot behavior that shows the dependence of strain rate, temperature, STZ population and dilatancy of systems. It reveals that the stress overshoots its steady state value due to the delayed activation of shear transformations that results from the insufficient free volume in the system. However, the subsequent strain softening (stress drop) is attributed to the shear-induced dilatation that is a result of the positive interplay between shear transformations and free volume creation, the latter playing the dominant role. Our analysis also demonstrates that the STZs, as basic carriers of amorphous plasticity, govern the yielding of the system, whereas the free volume dynamics significantly affects the post-yielding behaviors.

1. Introduction

Understanding of plasticity, i.e., how solids flow, is a classical problem (Hill, 1998), however it remains a challenge, particularly in the absence of a crystal lattice. Dislocation-mediated plasticity of crystals breaks down in the face of amorphous solids without long-range order (Falk, 2007; Chen, 2011). Regarding plastic flow of amorphous solids, ranging from glassy polymers to metallic glasses, a common feature is the stress overshoot (Hasan and Boyce, 1995; Kawamura et al., 1997; de Hey et al., 1998; Koumakis et al., 2012): the stress versus the applied strain first increases to a maximum and then decreases towards its steady-state value. The universality of this behavior implies that certain fundamental processes should underlie amorphous plasticity, albeit the diversity of microscopic constituents.

In the past few decades, theories concerning the plasticity of amorphous solids have developed along two main avenues. (i) The free-volume theory (Spaepen, 1977) argues that the plastic flow results from a series of stress-driven creation events of free volume via individual atomic jumps. (ii) The "shear transformation (ST)" theory (Argon, 1979) proposes that the basic carries of amorphous plasticity are irreversible rearrangements of small clusters of particles (i.e., atoms and molecules). However, an integrated picture for amorphous plasticity is emerging that (Falk and Langer, 1998; Langer, 2001; Lemaître, 2002; Argon and Demkowicz, 2008; Henits et al., 2012): free volume has a "catalytic" capability to trigger STs and meanwhile is enriched by the latter; free volume can be depleted by relaxation, which may cause potential STs to extinguish. Recently, Langer and co-workers (Langer, 2004; Bouchbinder et al., 2007a,b; Langer, 2008; Bouchbinder and Langer, 2009) have developed an athermal version of the shear-transformation-zone (STZ) theory where an

* Corresponding author at: State Key Laboratory of Nonlinear Mechanics, Institute of Mechanics, Chinese Academy of Sciences, Beijing 100190, China.
E-mail addresses: mqjiang@imech.ac.cn (M.Q. Jiang), lhdai@lnm.imech.ac.cn (L.H. Dai).

http://dx.doi.org/10.1016/j.mechmat.2014.10.002
0167-6636/

effective disorder temperature (analogous to the free volume in some sense) is introduced to directly relate with the STZ density. They revealed that the stress overshoot occurs due to a lack of the initial STZ density or effective disorder temperature in systems; new STZs must be generated by a stress higher than the steady state flow stress. This basic picture motivates us to further ask: what roles do the STs and free volume play, respectively, during the overshoot process? The present work attempts to answer this question. For this purpose, we propose a constitutive model for amorphous solids, within the framework of the classical STZ theory developed by Falk and Langer (1998).

2. Theoretical model

Consider an amorphous solid at temperatures T near the glass transition temperature T_g. The deformation is expected to be spatially homogeneous, modeled for a simple-shear case. The overall shear-strain rate $\dot{\varepsilon}$ can be decomposed into elastic and plastic parts, $\dot{\varepsilon} = \dot{\varepsilon}^{el} + \dot{\varepsilon}^{pl}$. The elastic deformation obeys Hooke's law $\sigma = \mu\varepsilon^{el}$, where σ is the shear stress and μ is the shear modulus. The plastic deformation results from the accumulation of unit STs occurring within local clusters (Argon, 1979; Falk and Langer, 1998; Johnson and Samwer, 2005; Jiang et al., 2009; Lemaître and Caroli, 2009). Here we adopt the mean-field approximation of STs, i.e., the STZ theory that ignores the spatial correlations between STs (Falk and Langer, 1998; Langer, 2001; Argon and Demkowicz, 2008; Lemaître and Caroli, 2009). Nevertheless, this assumption of spatial homogeneity is sufficient to capture the homogeneous flow of amorphous solids.

The core of the STZ theory (Falk and Langer, 1998; Langer, 2001) is that STZs, localized regions where potential STs take place, are two-state systems; they can switch forth and back between only two orientations. In the present simple-shear case, the two orientations correspond to the shear "positive" and "negative" directions, respectively. We denote the original state of a STZ as the "+" state, and its post-transformation state as the "−" state. Populations (number density) $n_{\pm}$ of two STZ states are natural order parameters to construct the constitution. Following Falk and Langer (1998) and Langer (2001), the plastic strain rate can be obtained by considering the dynamic balance of STs between "+" and "−" states:

$$\dot{\varepsilon}^{pl} = V_a(R_+ n_+ - R_- n_-), \tag{1}$$

where V_a is the STZ activation volume that is the product of characteristic STZ volume and shear strain, $R_{\pm}$ are the ST rates from a $\pm$ to a $\mp$ state. Equations of motion for the populations are (Falk and Langer, 1998; Langer, 2001):

$$\dot{n}_{\pm} = n_{\mp}R_{\mp} - n_{\pm}R_{\pm} + \bar{\varphi}\left|\sigma\dot{\varepsilon}^{pl}\right|(n_{\infty}/2 - n_{\pm}). \tag{2}$$

The first two terms on the right-hand side describe internal reconstructions between two STZ states. The last two terms in parentheses account for the rates of creation and annihilation of STZs, proportional to the plastic work rate $\left|\sigma\dot{\varepsilon}^{pl}\right|$ with a coefficient $\bar{\varphi}$. Physically, the plastic flow constantly agitates the particles, thus creating and destroying local configurations (Lemaître, 2002). Note that n_{∞} is the total populations of STZs generated in the system that is in a steady flow state.

For a low-temperature system, STs are free-volume or entropy activated, in which the applied stress is the driving force and the thermal activation is negligible (Falk and Langer, 1998; Bouchbinder et al., 2007a,b). However, as originally proposed by Argon that STs are stress-driven thermally activated events initiated around free volume regions (Argon, 1979), which is more applicable to our present thermal system. Actually, our recent work (Jiang et al., 2014) substantiates the idea that stress-driven STZs need thermal assistance, and further predicts that athermal or very-low-temperature STZs are prone to suffer a dilatation mode (we call it tension transformation zone, TTZ (Jiang et al., 2008)) due to their relatively low critical stress. Therefore we modify the ST rates to involve the internal dependence of free volume, thermal and stress fluctuations. First, only a particle group that resides in a "fertile" site with a typical free volume v^* has the possibility to transform. According to the free-volume theory (Cohen and Turnbull, 1959; Spaepen, 1977), the probability that a particle group is in this "fertile" site can be calculated as $\exp\left(-xv^*/v_f\right)$ where x is a geometrical factor, v_f is the free volume that the group surrounds. If no external stress is applied, subsequent STs are triggered by thermal activation across an energy barrier ΔG (Fig. 1). However the applied stress can tilt the activation energy barrier. Along the shear "positive" direction, the activation barrier from "+" to "−" becomes $\Delta G - \sigma V_a/2$; a backward activation should surmount the barrier $\Delta G + \sigma V_a/2$. Thus, the ST rates become:

$$R_{\pm} = \exp\left(-\frac{xv^*}{v_f}\right) f \exp\left(-\frac{\Delta G \mp \sigma V_a/2}{k_B T}\right), \tag{3}$$

where f is an attempt frequency, k_B is the Boltzmann constant. It must be pointed out that, in the present model, the free volume is not directly correlated to the STZ density, but definitely facilitates the STZ operations. In other words, the free volume (together with temperature and stress) directly influences the STs rates, instead of the absolute value of the STZ density. We believe that such a treatment

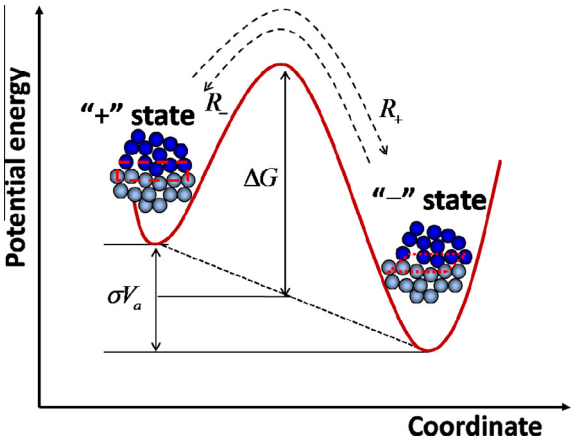

Fig. 1. Illustration of a shear transformation, the basic step for macroscopic plastic flow in amorphous solids.

has at least two merits. First, it can make sure that the STZs rather than the free volume are the main contribution to amorphous plasticity. In fact, the free volume indirectly affects the plastic deformation by making an impact on the operations of STZs. Second, since STZ density and free volume are not directly coupled, we could identify the liquid-like regions as the STZs. This agrees with the argument of Argon (1979) and Argon and Demkowicz (2008).

For amorphous systems such as metallic glasses, the lack of a long-range periodicity leads to the nanoscale heterogeneity in the distribution of the inherent defects, giving rise to the formation of densely packed clusters and loosely packed defective domains (Ichitsubo et al., 2005; Dmowski et al., 2010; Liu et al., 2011; Wagner et al., 2011). The former are usually called solid-like regions and the latter are liquid-like regions. These liquid-like regions can be regarded as the potential STZs that have a change to undergo the plastic deformation. However, whether a liquid-like region can be a true STZ or not depends on the free volume within the liquid-like region, the ambient temperature and the applied stress, as formulated in Eq. (3). For an "athermal" system well below T_g, it is expected that only a very small fraction of the liquid-like regions can become STZs (Bouchbinder et al., 2007b), because the plastic deformation is prone to be highly localized into nanoscale shear bands and even be restrained at sufficiently low temperatures (Li et al., 2013; Jiang et al., 2014). However, for a thermal system near T_g, the total deformation is spatially homogeneous. It is expected that most (or almost all) of liquid-like regions will be activated to be STZs as plasticity carriers. Many previous works (Ichitsubo et al., 2005; Argon and Demkowicz, 2008; Dmowski et al., 2010; Liu et al., 2011) have revealed that the fraction of liquid-like regions is of the order of 10^{-1}. Therefore, we reasonably assume that the present system has relatively higher density of STZs, as compared to the "athermal" case. One question naturally arises: does the basic spirit of the STZ theory that STZs interact very weakly with each other still hold for such a system?

For an "athermal" system, the STZs are rare and their interactions can be neglected due to large distance between STZs (Langer, 2004; Bouchbinder et al., 2007a,b). However, the interaction of STZs is not essentially determined by the number of STZs. It has been accepted that the STZ operations in an amorphous system can be treated as an Eshelby-type inclusion problem (Argon, 1979; Sun et al., 2010; Chattoraj and Lemaître, 2013). The operation of one STZ will give rise to an increment of elastic strain energy stored in the surrounding elastic medium, which triggers the activation of neighboring STZs. If the Eshelby elastic strain energy is too small to affect the neighboring STZs, we can still ignore the interaction of STZs, although the STZ number maybe is considerable. According to the Eshelby inclusion theory (Eshelby, 1957), the elastic strain energy is proportional to the elastic modulus of the medium and the STZ (activation) volume (Argon, 1979; Johnson and Samwer, 2005; Sun et al., 2010). With increasing temperature, the elastic modulus decreases, which becomes significant near T_g (Rouxel, 2007; Khonik et al., 2009), and at the same time, the STZ volume becomes smaller. Recently, Pan et al. (2011) have revealed that the STZ volume in metallic glasses can decrease by about one order of magnitude as the temperature increases from room temperature close to T_g. Therefore, for a thermal system near T_g such as our present case, the assumption that the STZs are irrelevant is still physical, and we believe that the STZ theory is still applicable.

The free volume dynamics must explicitly be taken into account in order to correctly describe the constitution. Generally, the time evolution of free volume is determined by a dynamic competition between flow-driven creation and relaxation-mediated annihilation (Spaepen, 1977; Lemaître, 2002). The former stems from Reynolds' dilatancy mechanism inherent to amorphous systems (Reynolds, 1885). A dense-random-packed system usually dilates, that is it expands in volume, as it is sheared (Dyre, 2006; Jiang and Dai, 2007; Keryvin et al., 2008). The average dilatancy (or the net created free-volume) can be estimated by considering the conversion of a fraction of the shear plastic energy into the bulk energy (Lemaître, 2002): $P^*\delta v_f = \bar{D}_{ia}\sigma\delta\varepsilon^{pl}$, where P^* is a characteristic pressure, $\bar{D}_{ia}$ is a dilatancy factor measuring the free volume creation ability of a system. A similar treatment has been performed by de Hey et al. (1998) and Heggen et al. (2005). Free-volume annihilation consists of a series of diffusion processes usually by means of two modes (Faupel et al., 2003; Huang et al., 2011; Bünz and Wilde, 2013): single-atom jump, or collective motion of atoms. However, many works (Faupel et al., 1990; Tang et al., 1999; Zollmer et al., 2002) confirms that the collective motion is the dominant process. Since the diffusion is thermally activated, the underlying collective motions can be regarded as the STs only activated by the thermal fluctuation (Fig. 1), called thermal transformations (TTs). Thus the annihilation rate of free volume equals the product of the amount of free volume annihilated per TT and the number of TTs per second. It is reasonably assumed that each TT can deplete a free volume that is proportional to v^* with a coefficient $\bar{\phi}$ (Bünz and Wilde, 2013). The number of TTs per second is actually the ST rate $R_{\pm}(\sigma = 0)$ without the external stress. The free volume dynamics therefore can be expressed as:

$$\dot{v}_f = -\bar{\phi}v^* \exp\left(-\frac{xv^*}{v_f}\right) f \exp\left(-\frac{\Delta G}{k_B T}\right) + \bar{D}_{ia}\frac{|\sigma\dot{\varepsilon}^{pl}|}{P^*}. \tag{4}$$

Note that the annihilation term is formally similar to that obtained by Spaepen (1977). Yet the physical meaning is different; here, the annihilation term describes the relaxation of free volume via TTs rather than single-atom jumps. Now free volume is not just a free parameter, but it is the third order-parameter.

As treated by Falk and Langer (1998), Langer (2001) and Steif et al. (1982), we define dimensionless order parameters

$$\Delta = \frac{n_- - n_+}{n_\infty}, \quad \Lambda = \frac{n_- + n_+}{n_\infty}, \quad \xi = \frac{v_f}{xv^*}. \tag{5}$$

These quantities actually are the internal state variables of the system. Δ and Λ represent, respectively, the bias and summation of normalized populations of two STZ states. ξ is the average free-volume concentration. To facilitate

the understanding of the numerical results, we normalize the temperature by T_g, stress and modulus by $\sigma_0 = 2k_BT_g/V_a$, time by $t_0 = f^{-1}\exp(\Delta G/k_BT_g)$, and strain by $\varepsilon_0 = V_a n_\infty$. After these, we obtain the dimensionless constitutive equations:

$$\dot{\varepsilon}^{pl} = \exp\left(-\frac{1}{\xi}\right)\exp\left[E_A\left(1-\frac{1}{T}\right)\right]\left[\Lambda\sinh\left(\frac{\sigma}{T}\right) - \Delta\cosh\left(\frac{\sigma}{T}\right)\right], \tag{6}$$

$$\dot{\sigma} = \varepsilon_0\mu\left(\dot{\varepsilon} - \dot{\varepsilon}^{pl}\right), \tag{7}$$

$$\dot{\Delta} = 2\dot{\varepsilon}^{pl} - \varphi\left|\sigma\dot{\varepsilon}^{pl}\right|\Delta, \tag{8}$$

$$\dot{\Lambda} = \varphi\left|\sigma\dot{\varepsilon}^{pl}\right|(1-\Lambda), \tag{9}$$

$$\dot{\xi} = D_{ia}\left|\sigma\dot{\varepsilon}^{pl}\right| - \phi\exp\left(-\frac{1}{\xi}\right)\exp\left[E_A\left(1-\frac{1}{T}\right)\right], \tag{10}$$

where $\varphi = \sigma_0\varepsilon_0\bar{\varphi}$, $D_{ia} = \bar{D}_{ia}\sigma_0\varepsilon_0/P^*$, $\phi = \bar{\phi}/x$, and $E_A = \Delta G/k_BT_g$. It must be addressed that all variables in these equations are non-dimensional, although the same notations are used as for their dimensional counterparts. The current constitutive model can describe not only a "start-up" experiment where a constant strain rate $\dot{\varepsilon}$ is applied, but also a constant stress (creep) experiment and even a natural aging process ($\sigma = 0$). The latter has been extensively studied by Langer (2001) and Lemaître (2002) based on the STZ theory. Here we devote our attentions to the "start-up" experiment, because the stress overshoot is the main interest of this paper. Furthermore, we focus on two rate processes which are

$$\begin{aligned} \mathrm{Cr}_\Lambda &= \frac{\partial\dot{\Lambda}}{\partial\Lambda}, \\ \mathrm{Cr}_\xi &= \frac{\partial\dot{\xi}}{\partial\xi}. \end{aligned} \tag{11}$$

The former characterizes the rate of increase of STZ populations that reflects the development degree of STs in the system, and the latter characterizes the net creation rate of free volume. This allows for a quantitative comparison of the dynamic processes of STZs and free volume on the same timescale.

3. Results and discussion

We take a typical $Zr_{41.2}Ti_{13.8}Cu_{12.5}Ni_{10}Be_{22.5}$ (Vitreloy 1) metallic glass as a model material for numerical calculations. The mechanical and physical parameters of the Vitreloy 1 metallic glass are derived from recent literatures (Lemaître, 2002; Johnson and Samwer, 2005; Johnson et al., 2007; Jiang and Dai, 2009; Cheng and Ma, 2011) and listed in Table 1. Using these parameters, Eqs. (6)–(10) can be numerically integrated at a fixed strain rate and a fixed temperature for an initial system (Δ_0, Λ_0 and ξ_0). In the following, all calculations are under quasi-static strain rates; thus the temperature rise is expected to be negligible (Zhang et al., 2007). Such an isothermal treatment has been widely adopted (Spaepen, 1977; Steif et al., 1982; Huang et al., 2002; Lemaître, 2002), which is helpful to highlight the essential physics. If there is no specific state, the initial system is chosen as: $\Delta_0 = 0$, $\Lambda_0 = 0.5$ and $\xi_0 = 0.05$ with a dilatancy factor $D_{ia} = 0.01$. Based on the obtained solutions, the two rate processes Cr_Λ and Cr_ξ defined by Eq. (11) can be further calculated.

First we apply the constitutive model to test its prediction ability for the stress overshoot. The numerical results are presented in Fig. 2, where the initial system is sheared at $\dot{\varepsilon} = 1\ \mathrm{s}^{-1}$ and $T = 0.9T_g$. Very clearly, the stress overshoot and subsequent strain softening (stress drop) can be predicted. It is found that the stress overshoot from the steady-state stress σ_∞ to the peak stress σ_{peak} corresponds to a remarkable increase of the plastic strain-rate $\dot{\varepsilon}^{pl}$ from zero to the applied strain-rate $\dot{\varepsilon}$ (the "A" section in Fig. 2(a)). Fig. 2(b) and (c) unveil that the plasticity growth is accompanied by a fast increase of the state variables Δ, Λ and ξ. A further comparison of three closely related rate processes: $\dot{\varepsilon}^{pl}$, Cr_Λ and Cr_ξ, is shown in Fig. 2(d). It is interesting to note that the three rate processes start up, respectively, in a time sequence: Cr_Λ, $\dot{\varepsilon}^{pl}$ and Cr_ξ. Moreover, the peak Cr_Λ is almost two times of that of Cr_ξ, indicating that the former is much faster than the latter. These results indicate that the development of amorphous plasticity is dominated by STZs, but assisted by the free volume. A more precise picture is that: for a system initially having a deficiency in free volume relative to that of the eventual flow state, a higher shear stress relative to σ_∞ is needed to activate STs firstly, and then plasticity grows, resulting in a creation of free volume; the created free-volume in turn fertilizes STs that further contribute to plasticity. Once $\dot{\varepsilon}^{pl} > \dot{\varepsilon}$, according to Eq. (7), the shear stress starts to decrease; but benefiting from the high level of free volume, the STs-mediated plasticity $\dot{\varepsilon}^{pl}$ further increases, forcing the stress to further decrease. The significant drop of stress eventually slows down the free volume creation that is balanced by its relaxation at

Table 1
Mechanical and physical parameters of Vitreloy 1 metallic glass.

Parameters	Notation	Value
Shear modulus	μ	35.3 GPa
STZ attempt frequency	f	$\sim 10^{13}$Hz
Glass transition temperature	T_g	625 K
STZ activation volume	V_a	$\sim$0.1 nm^3
STZ activation energy	ΔG	$\sim$1 eV
Steady-state populations of STZ	n_∞	V_a^{-1}
Ratio of the coefficient $\bar{\phi}$ and the geometrical factor x	ϕ	10
Proportional coefficient between STZ-creation/annihilation rate and plastic work rate	φ	0.5

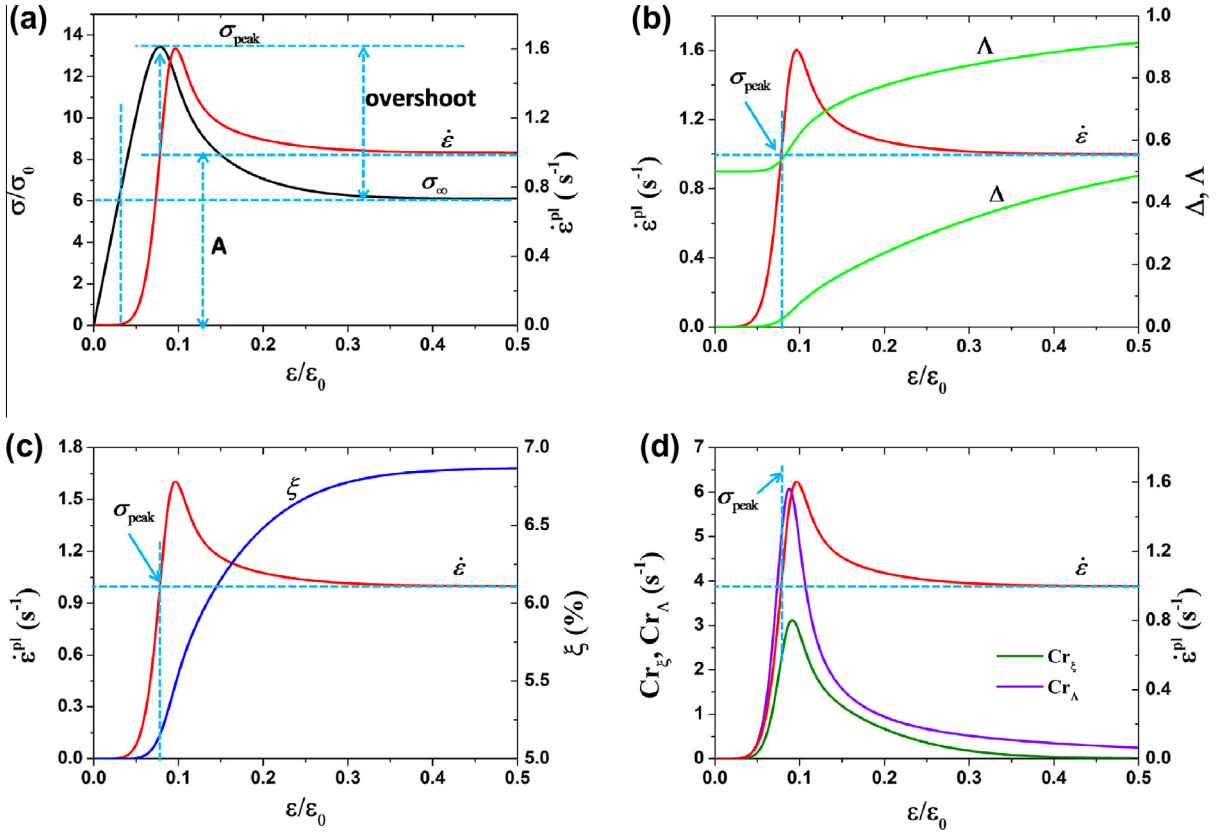

Fig. 2. Constitutive behavior of an amorphous solid at $\dot{\varepsilon} = 1\ s^{-1}$ and $T = 0.9T_g$: (a) normalized shear stress σ/σ_0 and plastic strain rate $\dot{\varepsilon}^{pl}$, (b) state variables Δ and Λ, (c) free volume concentration ξ, and (d) Cr_Λ and Cr_ξ versus normalized shear strain $\varepsilon/\varepsilon_0$.

the steady state; at that moment, the shear stress also reaches its steady state. However, the extinguishment of STs is delayed and the STZ populations will saturate into the steady state value only in the long-time limit. These results reveal that the free volume dynamics determines when the plastic flow reaches its steady state, although the plasticity is dominated by STZs. For the stress overshoot, we can draw a primary conclusion that, at a given strain rate and an ambient temperature, the stress overshoot occurs due to the delayed activation of STs that results from the insufficient free volume in systems; the free-volume creation via STs will, in turn, decrease the high stress (up to σ_{peak}) back to σ_∞, resulting in a pronounced strain softening. The stress overshoot and the subsequent strain softening always appear together. This conclusion is consistent with the stress overshoot picture proposed by Bouchbinder et al. (2007a,b) and Langer (2008).

The constitutive model can also capture the strain-rate and temperature dependence of stress overshoots, which are shown in Figs. 3 and 4, respectively. The results exhibit some qualitative agreement with experiments (Hasan and Boyce, 1995; Kawamura et al., 1997, 2012; de Hey et al., 1998; Zhang et al., 2013). The higher the strain rates or the lower the temperatures, the more pronounced stress overshoots occur. The overshoot mechanism is consistent with that revealed in Fig. 2. Under higher strain rates, a higher stress can be reached within the same loading time (Fig. 3(a)), thus triggering faster STs (indicated by Δ and Λ in Fig. 3(b)) and consequently plasticity develops faster (Fig. 3(c)). More free volume can be generated (Fig. 3(d)), which gives rise to a more pronounced strain softening (Fig. 3(a)). With increasing strain rate, the rates of both STs (Fig. 3(e)) and free volume creation (Fig. 3(f)) can reach higher peak values, implying that they prompt each other with a positive feedback in the present case. For very small strain rates, no overshoots occur. The reason is that the initial free volume decreases, rather than increases, to its steady-state value (Fig. 3(d)), corresponding to a negative net creation rate (see inset of Fig. 3(f)). The underlying physics is that the relaxation of free volume overwhelms (or is faster than) its creation due to very low rate of STs (Fig. 3(e)). With decreasing temperature, the new ST activations also need a higher stress or overshoot (Fig. 4(a)), resulting in a more and faster free-volume creation that directly contributes to the strain softening. The system's dynamics (see Fig. 4(b)–(f)) at lower temperatures is analogous to that at higher strain rates, thus obeying the time–temperature correspondence principle, as revealed previously (Jiang and Dai, 2009). Furthermore, following Falk et al. (2004), we generalize the present stress state to the uniaxial stress state. Then a quantitative comparison with the uniaxial experiments can be made, where we only focus on the homogeneous deformation data of the Vitreloy 1 at high temperatures and low strain rates reported

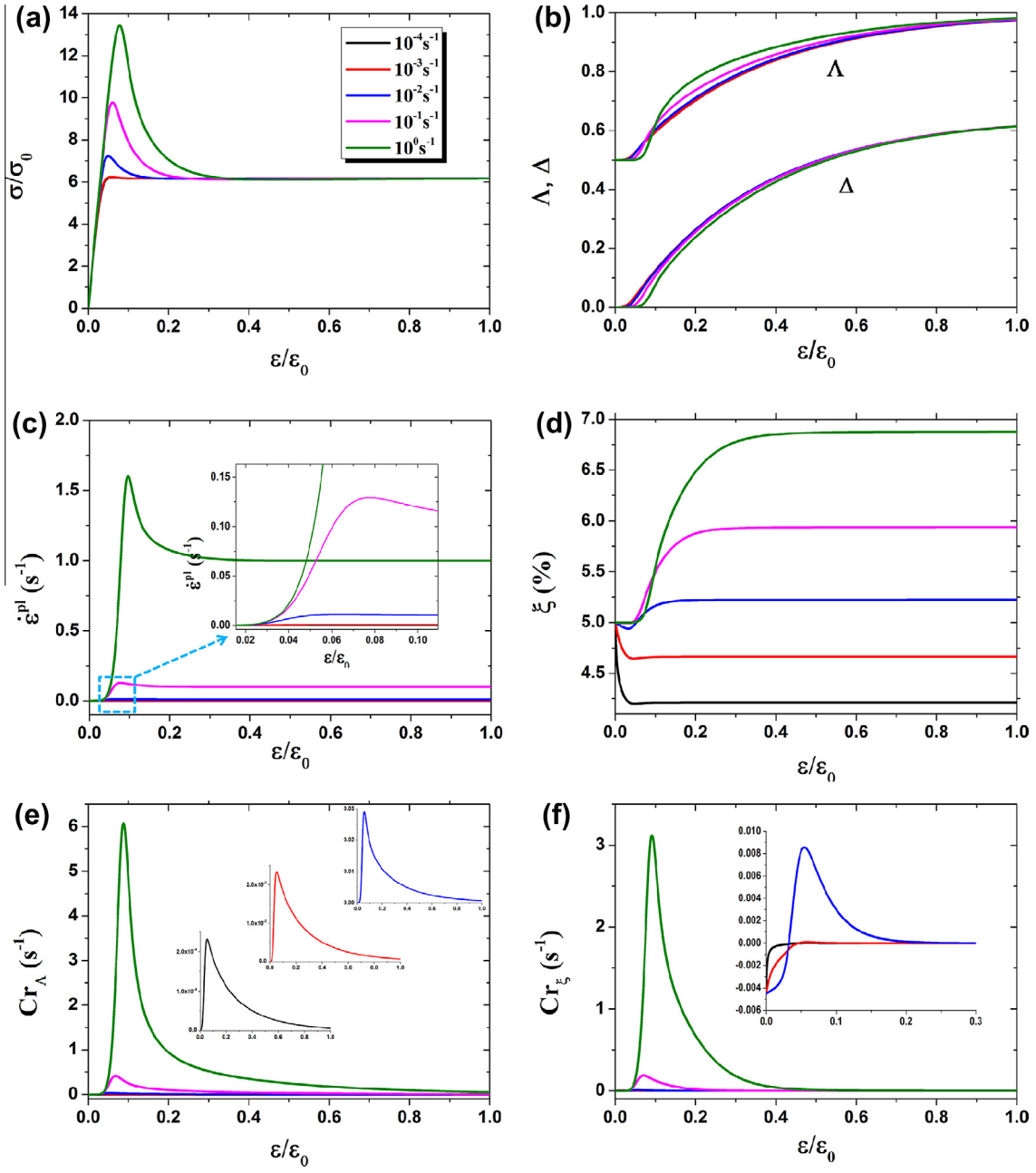

Fig. 3. Strain-rate dependence of constitutive behavior at $T = 0.9T_g$: (a) σ/σ_0, (b) Δ and Λ, (c) $\dot{\varepsilon}^{pl}$, (d) ξ, (e) Cr_Λ, and (f) Cr_ξ versus $\varepsilon/\varepsilon_0$.

by Lu et al. (2003). Fig. 5 shows that our theoretical model can well fit these experimental data of the Vitreloy 1. The agreement confirms the rationality and prediction capability of the present model.

Besides the strain-rate and temperature, the free-volume dynamics depends closely on the dilatancy of the system that is measured by D_{ia} (see Eq. (10)). Fig. 6(a) shows the stress–strain curves for different values of D_{ia}, all calculated for $\dot{\varepsilon} = 10^{-2}\ \mathrm{s}^{-1}$ and $T = 0.9T_g$. It is interesting to find that, with the decrease of D_{ia}, the plastic yielding behavior shows a gradual transition from stress overshoot (strain softening) to strain hardening. For the system having larger dilatancy, the plasticity $\dot{\varepsilon}^{pl}$ can develop into a higher level before the decline to its steady state (Fig. 6(b)). This behavior results from the more drastic STs (Fig. 6(c)) that are assisted by the faster free-volume creation (Fig. 6(d)). The larger the system's dilatancy, the more precipitous and narrower the peaks of both ST and free volume creation rates (Fig. 6(e) and (f)), corresponding to a more pronounced strain softening. In the system with very low dilatancy, the free volume dynamics is dominated by the relaxation process, leading to a constantly decrease of free

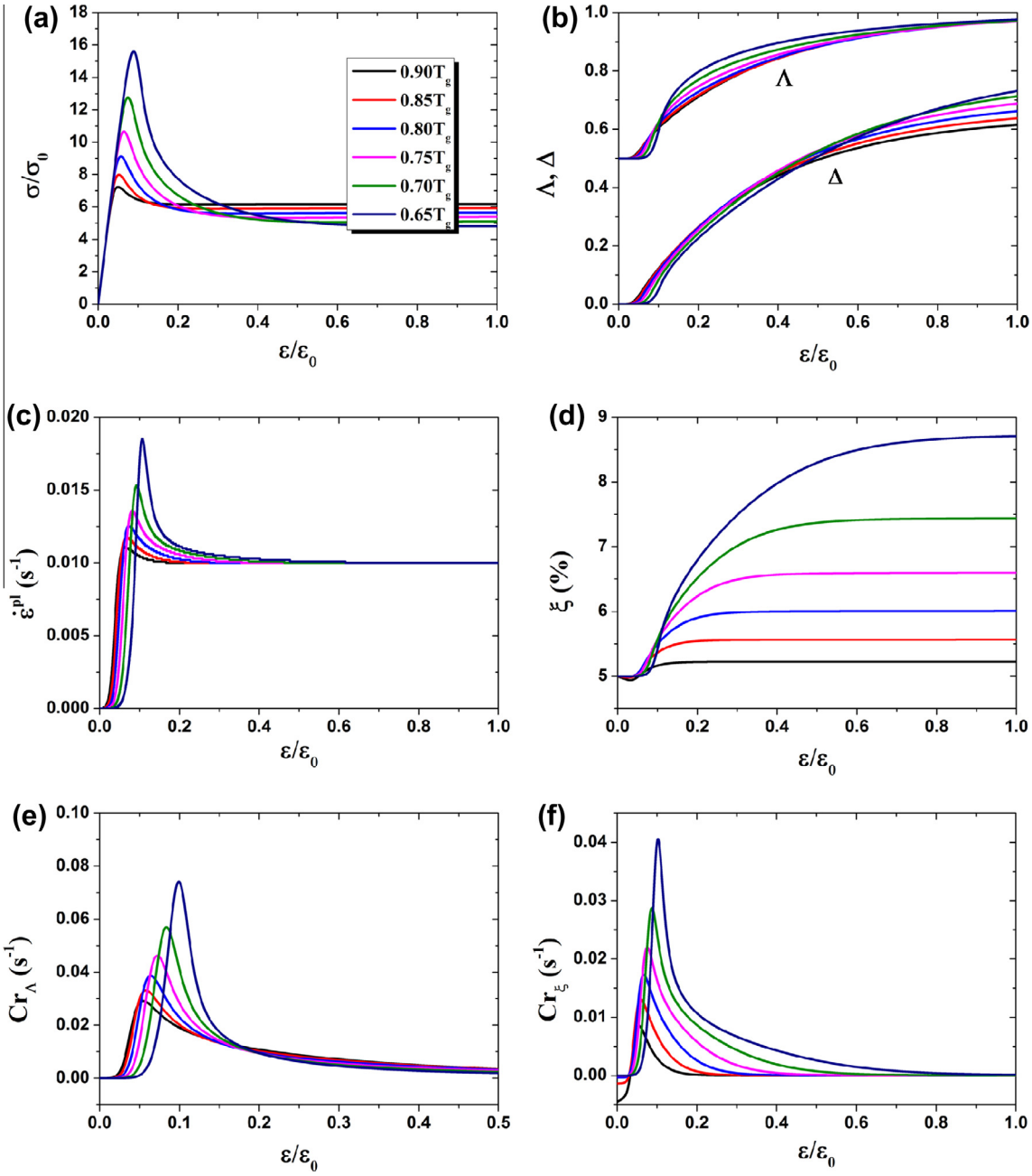

Fig. 4. Temperature dependence of constitutive behavior at $\dot{\varepsilon} = 10^{-2}$ s^{-1}: (a) σ/σ_0, (b) Δ and Λ, (c) $\dot{\varepsilon}^{pl}$, (d) ξ, (e) Cr_Λ, and (f) Cr_ξ versus $\varepsilon/\varepsilon_0$.

volume (Fig. 6(d)) without a steady state. This behavior corresponds to a negative net creation rate of free volume (see the inset of Fig. 6(f)). The decrease of free volume after yielding results in a considerable increase of the stress (strain hardening). This mechanism for strain hardening agrees well with our previous result (Jiang and Dai, 2009) within the free volume theory coupled by a thermal effect. The results shown in Fig. 6 further confirm that the free volume dynamics significantly affects the post-yielding behavior of the system, although the yielding is essentially governed by the STs.

We also investigated the dependence of the stress overshoot on the initial STZ population Λ_0. A larger Λ_0 corresponds to a more liquid-like system, and vice versa (Falk et al., 2004). Here we assume that the range of Λ_0 is compared to the liquid-like fraction in metallic glasses. The exact relationship between the STZ density and the liquid-like fraction is beyond the scope of the present investigation. Fig. 7(a) shows the stress–strain curves of the systems by varying Λ_0 from 0.1 to 1, where a large dilatancy factor $D_{ia} = 0.01$ is adopted. It can be seen that all systems exhibit stress overshoots of prominence,

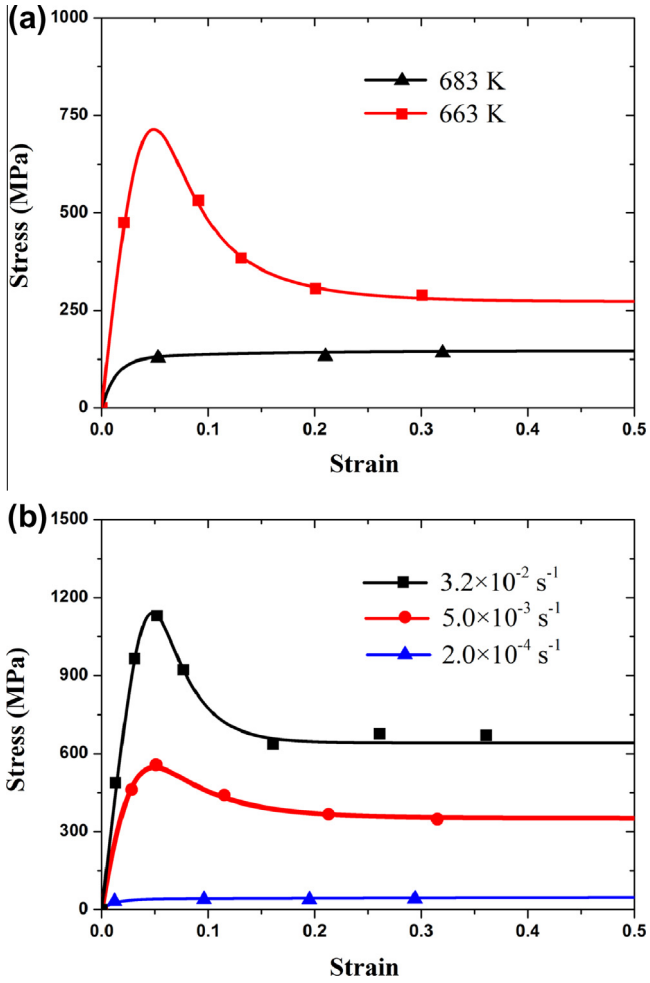

Fig. 5. Theoretical stress–strain curves (solid lines) compared to the uniaxial experimental data (symbols) reported by Lu et al. (2003).

decreasing with increasing Λ_0. More solid-like systems need a higher stress to activate STs with a higher rate (Fig. 7(b)). The large dilatancy guarantees the creation of free volume always with a positive rate (Fig. 7(c)), resulting in the occurrence of strain softening. It is noteworthy that, in the fully liquid-like system ($\Lambda_0 = 1$), although no STZ population is created (Fig. 7(b)), internal reconstructions between two STZ states still have the ability to generate free volume due to the sufficiently large dilatancy. This result is helpful to understand the simulation of Argon and Demkowicz (2008), and they found that the stress still shows the overshoot for the case that the liquid fraction is nearly equal to its steady state value. The reason is maybe due to the STZs' reconstructions and the resulting free volume creation. However, usually the more liquid-like a system, the smaller its dilatancy ability, since such a system is very susceptible to shear deformation without changing its volume. Therefore, for the large Λ_0 cases, the yielding behaviors should correspond to those cases in Fig. 7(d) where a small dilatancy factor $D_{ia} = 0.001$ is applied, although the precise relationship between Λ_0 and D_{ia} is unknown. For these systems (large Λ_0 and small D_{ia}), strain hardening can be predicted, which is still attributed to the free volume annihilation (Fig. 7(f)). The underlying mechanism is the very limited ability of systems to dilate or to create free volume, and on the other hand, the lower ST rates (Fig. 7(e)) relative to those in the larger dilatancy cases (Fig. 7(b)).

4. Transition from jammed to flowing states

One of the most intriguing features of the STZ theory is that a yield stress naturally emerges from its basic structure (Falk and Langer, 1998; Lobkovsky and Langer, 1998; Langer and Lobkovsky, 1999; Langer and Lobkovsky, 1999). It is therefore interesting to reexamine this feature in the present STZ-based model, especially with the participation of the free volume dynamics. Our model, i.e., Eqs. (6)–(10), can also exhibit explicitly an exchange of dynamic stability between jammed and flowing states (see Fig. 2), however the present situation is more complicated with some unexpected results.

In the first (jammed) state, the system has a viscoelastic solution in which the plastic strain rate is zero, and we have

$$\Lambda = \Lambda_0, \quad \Delta = \Lambda \tanh\left(\frac{\sigma}{T}\right). \tag{12}$$

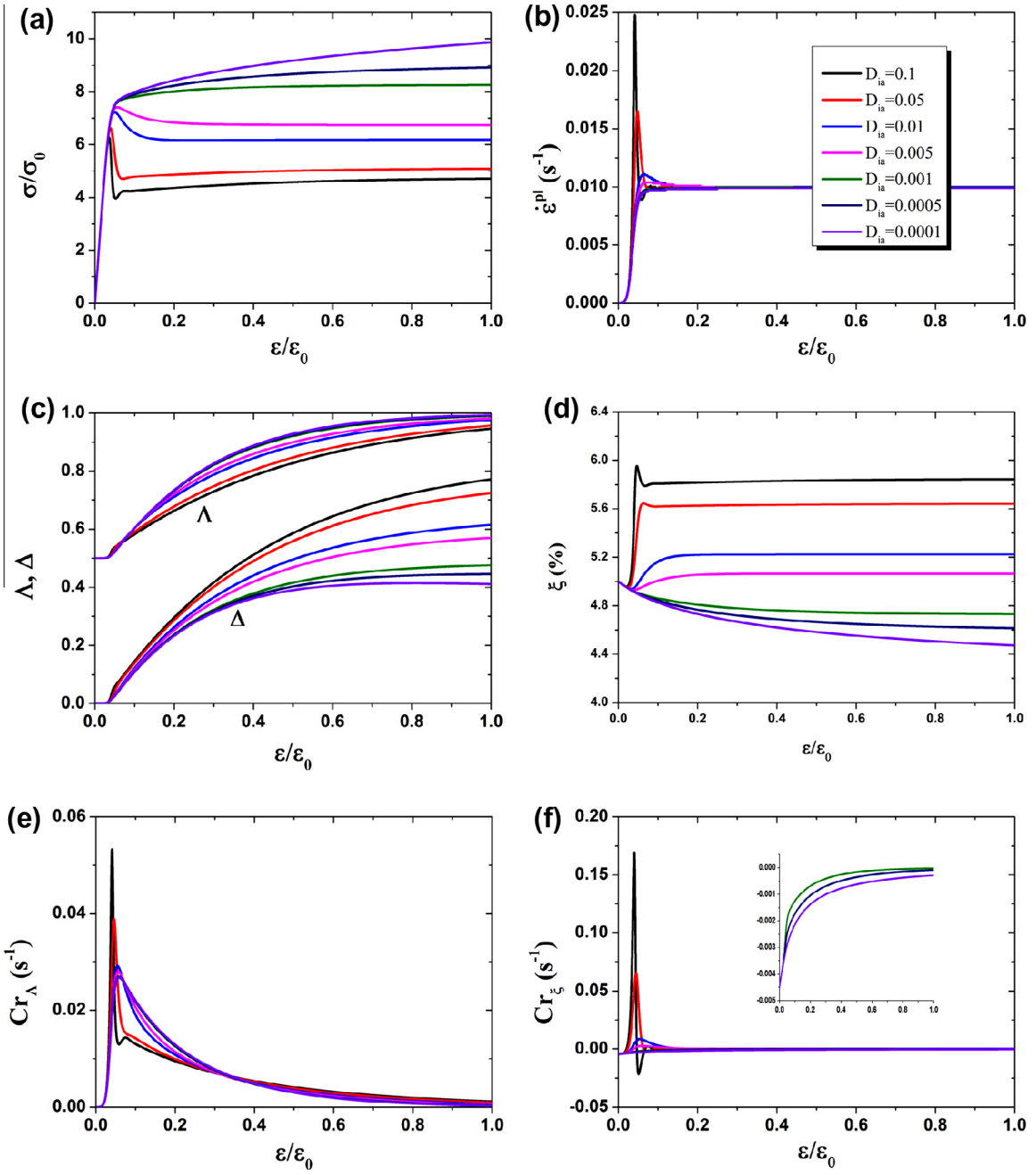

Fig. 6. Dilatancy dependence of constitutive behavior at $\dot{\varepsilon} = 10^{-2}$ s^{-1} and $T = 0.9T_g$: (a) σ/σ_0, (b) $\dot{\varepsilon}^{pl}$, (c) Δ and Λ, (d) ξ, (e) Cr_Λ, and (f) Cr_ξ versus $\varepsilon/\varepsilon_0$.

Note that there is an intrinsic relaxation of free volume in the jammed state (see Eq. (10) if $\dot{\varepsilon}^{pl} = 0$). In the second (flowing) state, the solution is viscoplastic, where $\dot{\varepsilon}^{pl} \neq 0$. Our present system exhibits a unique feature. That is, when the stress reaches its steady state, the STZ states (both Λ and Δ) do not simultaneously and immediately come into their respective steady states. That means that the relaxation of the flow stress to the steady state is faster than the rate at which the STZ density evolves into its steady state value. For example, we can see the 10^{-4} s^{-1} case in Fig. 3, where the jammed-to-flowing transition is more obvious due to no stress overshoot. It is found that at the moment when the steady state flow sets in, the STZ density Λ is only about 0.60. The result compares with the simulations of Shi and Falk (2005). They found that in a homogeneously deforming glass the deformation participation ratio can be approximately 0.50. Therefore, only for the long-time and sustained steady state homogeneous flow, we have

$$\Lambda = \Lambda_0 \to 1, \quad \Delta = \Delta_0 \to \frac{2}{\varphi\sigma}. \tag{13}$$

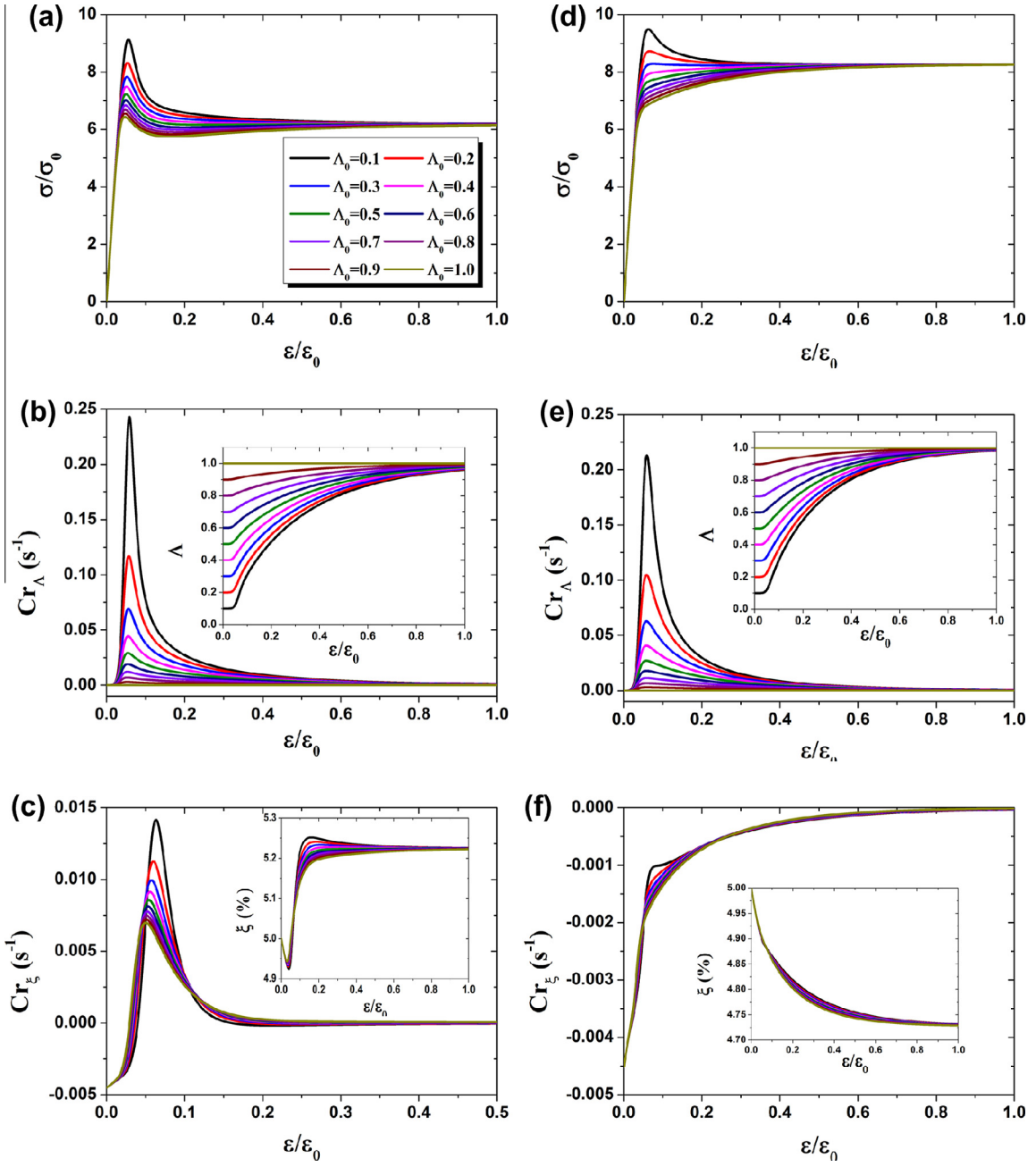

Fig. 7. STZ-population Λ_0 dependence of constitutive behavior at $\dot{\varepsilon} = 10^{-2}$ s^{-1} and $T = 0.9T_g$. (a) and (d) σ/σ_0, (b) and (e) Cr_Λ, (c) and (f) Cr_ξ versus $\varepsilon/\varepsilon_0$. The insets of (b) and (e) show the Λ versus $\varepsilon/\varepsilon_0$. The insets of (c) and (f) show the ξversus $\varepsilon/\varepsilon_0$. Left panel: $D_{ia} = 0.01$; right panel: $D_{ia} = 0.001$.

However, the free volume shows no the time delay; the stress and the free volume simultaneously come into their respective steady states. Then we obtain an additional relation,

$$\sigma[\Lambda \sinh(\sigma/T) - \Delta \cosh(\sigma/T)] = \frac{\phi}{D_{ia}}. \tag{14}$$

It is noted that there are two crossovers between the two solutions, but which determines the intrinsic yield stress needs further analysis. The first crossover occurs when both Eqs. (12) and (14) are satisfied. However, we find that this situation has no solutions, which again confirms that the plastic yielding of the system is not controlled by the free volume. The second occurs when both Eqs. (12) and (13) are satisfied. In this case, the yield stress is determined by

$$\Lambda_0 \tanh\left(\frac{\sigma_y}{T}\right) \to \frac{2}{\varphi\sigma_y}. \tag{15}$$

We find that if and only if $\Lambda_0 \approx 2/3$, not unity, the yield stress $\sigma_y \approx 6$ (actually $6\sigma_0$) near the glass transition temperature ($T \approx 1$), which is consistent with the numerical results. Eq. (15) describes an interesting phenomenon, that is, the value of Λ at the yield point is just equal to the saturation value of Δ in the long-time limit, because $\tanh(\sigma_y/T) \approx 1$ for the present system. Based on the above analysis, we provide further evidence that the plastic yielding of systems is inherently governed by the STZ operations, albeit the participation of free volume.

5. Conclusion

Taking the interaction of STs and free volume dynamics into account, constitutive equations for amorphous plasticity are developed along the lines of the classical STZ theory. A striking feature of the present model is that the free volume (together with the temperature and stress) directly influences the ST rates, instead of the absolute density of STZs. This constitutive model can capture various plastic yielding behaviors including stress overshoot, strain softening and hardening. The stress overshoot occurs mainly due to a deficiency in the initial free volume that slows down the creation rate of STZs. As a result, a higher stress than its steady state value is needed to activate new STZs. After that, the higher stress will drop as STs-mediated flow induces a fast creation of free volume, showing a strain softening. The strain hardening is due to a constant relaxation of free volume via TTs after yielding. Our analysis demonstrates that the stress overshoot phenomena is not directly related to the initial STZ density, but is closely determined by the dynamic operations of STZs. Finally, the intrinsic transition from jammed to flowing states is reexamined within the present model. It is revealed that the plastic yielding is inherently controlled by STZ operations, although the post-yielding behaviors strongly depend on the free volume dynamics. We believe that these results may increase the understanding of plasticity mechanism of amorphous solids, and have useful implications for designing amorphous materials (e.g. metallic glasses) with desired mechanical properties.

Acknowledgments

This work was supported by the National Nature Science Foundation of China (Grant Nos 11372315, 11132011 and 11023001) and the National Key Research Program of China (Grant No 2012CB937500). MQJ acknowledges the Alexander von Humboldt Foundation for support with a research fellowship. GW acknowledges the support by DFG. LHD acknowledges the CAS/SAFEA International Partnership Program for Creative Research Teams.

References

Argon, A.S., 1979. Plastic deformation in metallic glasses. Acta Metall. 27, 47–58.
Argon, A.S., Demkowicz, M.J., 2008. What can plasticity of amorphous silicon tell us about plasticity of metallic glasses? Metall. Mater. Trans. A 39A, 1762–1778.
Bouchbinder, E., Langer, J.S., 2009. Nonequilibrium thermodynamics of driven amorphous materials. II. Effective-temperature theory. Phys. Rev. E 80, 031132.
Bouchbinder, E., Langer, J.S., Procaccia, I., 2007a. Athermal shear-transformation-zone theory of amorphous plastic deformation. I. Basic principles. Phys. Rev. E 75, 036107.
Bouchbinder, E., Langer, J.S., Procaccia, I., 2007b. Athermal shear-transformation-zone theory of amorphous plastic deformation. II. Analysis of simulated amorphous silicon. Phys. Rev. E 75, 036108.
Bünz, J., Wilde, G., 2013. Direct measurement of the kinetics of volume and enthalpy relaxation of an Au-based bulk metallic glass. J. Appl. Phys. 114, 223503.
Chattoraj, J., Lemaître, A., 2013. Elastic signature of flow events in supercooled liquids under shear. Phys. Rev. Lett. 111, 066001.
Chen, M.W., 2011. A brief overview of bulk metallic glasses. NPG Asia Mater. 3, 82–90.
Cheng, Y.Q., Ma, E., 2011. Intrinsic shear strength of metallic glass. Acta Mater. 59, 1800–1807.
Cohen, M.H., Turnbull, D., 1959. Molecular transport in liquids and glasses. J. Chem. Phys. 31, 1164–1169.
de Hey, P., Sietsma, J., van den Beukel, A., 1998. Structural disordering in amorphous Pd40Ni40P20 induced by high temperature deformation. Acta Mater. 46, 5873–5882.
Dmowski, W., Iwashita, T., Chuang, C.P., Almer, J., Egami, T., 2010. Elastic heterogeneity in metallic glasses. Phys. Rev. Lett. 105, 205502.
Dyre, J.C., 2006. Colloquium: the glass transition and elastic models of glass-forming liquids. Rev. Mod. Phys. 78, 953–972.
Eshelby, J.D., 1957. The determination of the elastic field of an ellipsoidal inclusion, and related problems. Proc. R. Soc. London, A 241, 376–396.
Falk, M.L., 2007. Materials science – the flow of glass. Science 318, 1880–1881.
Falk, M.L., Langer, J.S., 1998. Dynamics of viscoplastic deformation in amorphous solids. Phys. Rev. E 57, 7192–7205.
Falk, M.L., Langer, J.S., Pechenik, L., 2004. Thermal effects in the shear-transformation-zone theory of amorphous plasticity: comparisons to metallic glass data. Phys. Rev. E 70, 011507.
Faupel, F., Huppe, P.W., Rätzke, K., 1990. Pressure-dependence and isotope effect of self-diffusion in a metallic-glass. Phys. Rev. Lett. 65, 1219–1222.
Faupel, F., Frank, W., Macht, M.P., Mehrer, H., Naundorf, V., Ratzke, K., Schober, H.R., Sharma, S.K., Teichler, H., 2003. Diffusion in metallic glasses and supercooled melts. Rev. Mod. Phys. 75, 237–280.
Hasan, O.A., Boyce, M.C., 1995. A constitutive model for the nonlinear viscoelastic viscoplastic behavior of glassy-polymers. Polym. Eng. Sci. 35, 331–344.
Heggen, M., Spaepen, F., Feuerbacher, M., 2005. Creation and annihilation of free volume during homogeneous flow of a metallic glass. J. Appl. Phys. 97, 033506.
Henits, P., Revesz, A., Kovacs, Z., 2012. Free volume simulation for severe plastic deformation of metallic glasses. Mech. Mater. 50, 81–87.
Hill, R., 1998. The Mathematical Theory of Plasticity. Oxford University Press, Oxford.
Huang, R., Suo, Z., Prevost, J.H., Nix, W.D., 2002. Inhomogeneous deformation in metallic glasses. J. Mech. Phys. Solids 50, 1011–1027.
Huang, X., Ling, Z., Zhang, H.S., Ma, J., Dai, L.H., 2011. How does spallation microdamage nucleate in bulk amorphous alloys under shock loading? J. Appl. Phys. 110, 103519.
Ichitsubo, T., Matsubara, E., Yamamoto, T., Chen, H.S., Nishiyama, N., Saida, J., Anazawa, K., 2005. Microstructure of fragile metallic glasses inferred from ultrasound-accelerated crystallization in Pd-based metallic glasses. Phys. Rev. Lett. 95, 245501.
Jiang, M.Q., Dai, L.H., 2007. Intrinsic correlation between fragility and bulk modulus in metallic glasses. Phys. Rev. B 76, 054204.
Jiang, M.Q., Dai, L.H., 2009. On the origin of shear banding instability in metallic glasses. J. Mech. Phys. Solids 57, 1267–1292.
Jiang, M.Q., Ling, Z., Meng, J.X., Dai, L.H., 2008. Energy dissipation in fracture of bulk metallic glasses via inherent competition between local softening and quasi-cleavage. Philos. Mag. 88, 407–426.
Jiang, M.Q., Wang, W.H., Dai, L.H., 2009. Prediction of shear-band thickness in metallic glass. Scr. Mater. 60, 1004–1007.
Jiang, M.Q., Wilde, G., Chen, J.H., Qu, C.B., Fu, S.Y., Jiang, F., Dai, L.H., 2014. Cryogenic-temperature-induced transition from shear to dilatational failure in metallic glasses. Acta Mater. 77, 248–257.
Johnson, W.L., Samwer, K., 2005. A universal criterion for plastic yielding of metallic glasses with a $(T/T_g)^{2/3}$ temperature dependence. Phys. Rev. Lett. 95, 195501.
Johnson, W.L., Demetriou, M.D., Harmon, J.S., Lind, M.L., Samwer, K., 2007. Rheology and ultrasonic properties of metallic glass-forming liquids: a potential energy landscape perspective. MRS Bull. 32, 644–650.

Kawamura, Y., Shibata, T., Inoue, A., Masumoto, T., 1997. Stress overshoot in stress–strain curves of Zr65Al10Ni10Cu15 metallic glass. Appl. Phys. Lett. 71, 779–781.
Keryvin, V., Crosnier, R., Laniel, R., Hoang, V.H., Sangleboeuf, J.C., 2008. Indentation and scratching mechanisms of a ZrCuAlNi bulk metallic glass. J. Phys. D. Appl. Phys. 41, 074029.
Khonik, V.A., Mitrofanov, Y.P., Lyakhov, S.A., Vasiliev, A.N., Khonik, S.V., Khoviv, D.A., 2009. Relationship between the shear modulus G, activation energy, and shear viscosity η in metallic glasses below and above T_g: direct in situ measurements of G and η. Phys. Rev. B 79, 132204.
Koumakis, N., Laurati, M., Egelhaaf, S.U., Brady, J.F., Petekidis, G., 2012. Yielding of hard-sphere glasses during start-up shear. Phys. Rev. Lett. 108, 098303.
Langer, J.S., 2001. Microstructural shear localization in plastic deformation of amorphous solids. Phys. Rev. E 64, 011504.
Langer, J.S., 2004. Dynamics of shear-transformation zones in amorphous plasticity: formulation in terms of an effective disorder temperature. Phys. Rev. E 70, 041502.
Langer, J.S., 2008. Shear-transformation-zone theory of plastic deformation near the glass transition. Phys. Rev. E 77, 021502.
Langer, J.S., Lobkovsky, A.E., 1999. Rate-and-state theory of plastic deformation near a circular hole. Phys. Rev. E 60, 6978–6983.
Lemaître, A., 2002. Rearrangements and dilatancy for sheared dense materials. Phys. Rev. Lett. 89, 195503.
Lemaître, A., Caroli, C., 2009. Rate-dependent avalanche size in athermally sheared amorphous solids. Phys. Rev. Lett. 103, 065501.
Li, G., Jiang, M.Q., Jiang, F., He, L., Sun, J., 2013. Temperature-induced ductile-to-brittle transition of bulk metallic glasses. Appl. Phys. Lett. 102, 171901.
Liu, Y.H., Wang, D., Nakajima, K., Zhang, W., Hirata, A., Nishi, T., Inoue, A., Chen, M.W., 2011. Characterization of nanoscale mechanical heterogeneity in a metallic glass by dynamic force microscopy. Phys. Rev. Lett. 106, 125504.
Lobkovsky, A.E., Langer, J.S., 1998. Dynamic ductile to brittle transition in a one-dimensional model of viscoplasticity. Phys. Rev. E 58, 1568–1576.
Lu, J., Ravichandran, G., Johnson, W.L., 2003. Deformation behavior of the Zr41.2Ti13.8Cu12.5Ni10Be2205 bulk metallic glass over a wide range of strain-rates and temperatures. Acta Mater. 51, 3429–3443.
Pan, D., Guo, H., Zhang, W., Inoue, A., Chen, M.W., 2011. Temperature-induced anomalous brittle-to-ductile transition of bulk metallic glasses. Appl. Phys. Lett. 99, 241907.
Reynolds, O., 1885. LVII. On the dilatancy of media composed of rigid particles in contact. With experimental illustrations. Philos. Mag. Ser. 5 (20), 469–481.
Rouxel, T., 2007. Elastic properties and short-to-medium-range order in glasses. J. Am. Ceram. Soc. 90, 3019–3039.
Shi, Y.F., Falk, M.L., 2005. Strain localization and percolation of stable structure in amorphous solids. Phys. Rev. Lett. 95, 095502.
Spaepen, F., 1977. A microscopic mechanism for steady state inhomogeneous flow in metallic glasses. Acta Metall. 25, 407–415.
Steif, P.S., Spaepen, F., Hutchinson, J.W., 1982. Strain localization in amorphous metals. Acta Metall. 30, 447–455.
Sun, L., Jiang, M.Q., Dai, L.H., 2010. Intrinsic correlation between dilatation and pressure sensitivity of plastic flow in metallic glasses. Scr. Mater. 63, 943–946.
Tang, X.-P., Geyer, U., Busch, R., Johnson, W.L., Wu, Y., 1999. Diffusion mechanisms in metallic supercooled liquids and glasses. Nature 402, 160–162.
Wagner, H., Bedorf, D., Kuchemann, S., Schwabe, M., Zhang, B., Arnold, W., Samwer, K., 2011. Local elastic properties of a metallic glass. Nat. Mater. 10, 439–442.
Zhang, H.W., Subhash, G., Maiti, S., 2007. Local heating and viscosity drop during shear band evolution in bulk metallic glasses under quasistatic loading. J. Appl. Phys. 102, 043519.
Zhang, M., Liu, L., Wu, Y., 2013. Facilitation and correlation of flow in metallic supercooled liquid. J. Chem. Phys. 139, 164508.
Zollmer, V., Rätzke, K., Faupel, F., Rehmet, A., Geyer, U., 2002. Evidence of diffusion via collective hopping in metallic supercooled liquids and glasses. Phys. Rev. B 65, 220201.